

Abstract

St. Olavs hospital has supplied a dataset of 2703 tissue samples at the tumor peripheral from ≈ 900 patients. NTNU want to examine all tissue samples with image processing to see if second harmonic generation microscope images of tissue can help classify cancer type (I, II, III) or in other words, cancer aggressiveness. This thesis documents a method which automates the microscope imaging of these tissue microarrays (TMA) and show how images can be structured and correlated to clinical data.

Automated microscope scanning is in principle straight forward, but the implementation is dependent on many aspects of the experimental setup. In general, some of the aspects discussed in this thesis are:

- Create image analysis algorithms that are robust to experimental variations.
- Correction of systematic errors like
 - intensity variations and
 - difference in coordinate systems of scanning raster patterns and stage movement.
- Automatic stitching of regular spaced images with variable degree of signal entropy in seams.
- Adjusting z-plane for large area samples with micrometer precision.

The aspects listed above are not unique to TMA-specimens and the experimental setup, and could be useful for similar projects. But the focus of the thesis will be on TMA and the experimental setup with a Leica SP8 microscope.

The conclusions are:

- Large area scans should adjust specimen plane to be at even distance to the objective to be time effective and avoid out of focus images.

- Using heuristics/constraints improves the reliability to automatic stitching algorithms, failing gracefully on images with little entropy in overlap.
- Leica LAS version 1.1.0.12420 have limited support for automatic microscopy, but it's possible to work around limitations to leverage fully automatic TMA-scanning.

Contents

Abstract	1
Preface	7
1 Introduction	9
2 Theory	13
Tissue microarrays	13
Scanning microscope	13
Image processing	16
Otsu thresholding	16
Spatial image filters	17
Sliding window filters	17
Image registration	17
Software	19
Leica LAS	19
CAM	19
XML	20
Scanning Template	21
OCR	21

Image formats	21
3 Methods	23
Microscope	23
Overview images	24
SHG images	25
Automated TMA scanning	25
Step 1: Collecting overview images	26
Step 2: Find specimen spots by segmentation	30
Step 3: Scanning each specimen spot	34
Alignment of z-plane	37
Correlating images with patient data	37
4 Discussion	41
Scanning	41
Rotation	43
Images and stitching	43
leicaexperiment	45
Segmentation	46
.	46
Stable stage insert	46
Leica LAS design	46
5 Conclusion	47
6 Appendix	49
Python software	49
Slide map errors	49

CONTENTS

5

References

53

Preface

Five years at NTNU have been a rollercoaster ride. Uphills at times, but also a great deal of fun. I'm grateful for the number of marvellous people I have met, the flexibility the student life brings, all the fun with the student society Spanskrøret and not to forget all the things I've learned.

A special thank you go to all the professors who share their knowledge every day, even at times when their students seems unmotivated.

The last year I have been warmly included in Magnus Borstad Lilledahl's research group, with Andreas Finnøy, Elisabeth Inge Romijn and Rajesh Kumar. It's been educational to work with them and exciting to get an insight in how they perform their work. Anna Bofin and Monica J. Engstrøm at St. Olavs has also been very welcoming, showing me histological patterns in tissues and provided the data set to my gratefulness. Thank you all!

I would also like to thank my family, who always have been supportive for the choices I've made. Lastly, the greatest thanks go to my life companion Yngvild, it wouldn't have been the same without you.

The future is already here, it's just not very evenly distributed. - William Gibson

Chapter 1

Introduction

With a population just above 5 million¹, three thousand women are diagnosed with breast cancer each year² in Norway. This makes breast cancer the most common kind of cancer, affecting one of every eleventh woman. Luckily breast cancer is often treatable, shown by the fatalities which was 649 in 2012². NTNU and St. Olavs hospital have been cooperating on research to find new ways to diagnose patients. The cooperation yielded a study on 37 subjects which showed positive results on difference of collagen structure from different parts of tumor tissue³. This thesis seeks to make it possible to expand the study from 37 subjects to the whole dataset available of ≈ 900 subjects.

The means to achieve the expanded dataset is to improve instrumentation by automate microscope imaging, with main focus on tissue microarrays. Tissue micro arrays are glass slides with samples arranged in a matrix pattern seen in figure 1.1. As tissue microarrays is standard procedure, not unique to breast cancer tissue, the work of this master is relevant for other studies too.

The tissue micro array shown in figure 1.1 is $\approx 24 \times 15$ mm in size. Using a moderate objective of 25x with 400×400 μm field of view, a single scan of the total dataset will be

$$\frac{24\text{mm}}{400\mu\text{m}} \cdot \frac{15\text{mm}}{400\mu\text{m}} = 2250 \text{ images.}$$

Depending on the precision of the microscope stage, images are not necessarily easily put together. Also, keeping microscope in focus for the whole surface can become challenging. Another approach would be not to scan the whole area in one scan, but to scan each of the

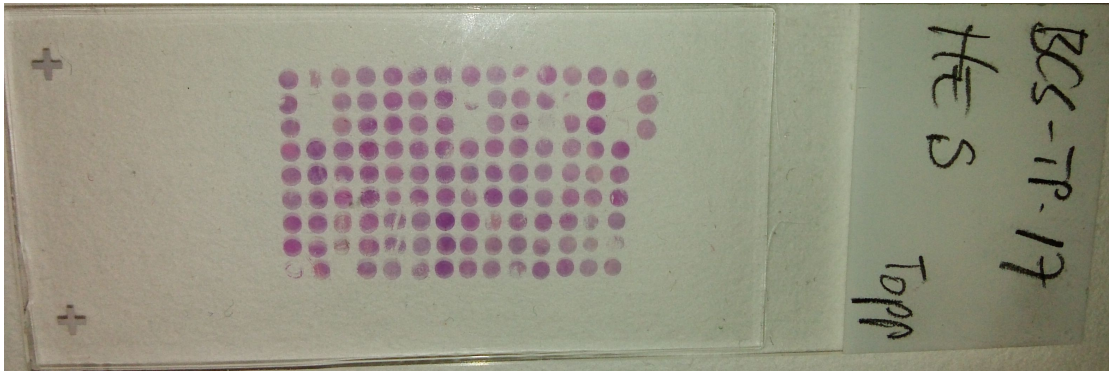


Figure 1.1: Tissue micro array of breast tissue at perifer of tumor. Three test samples are beside the array of 14x9 samples to avoid mix up of patients when rotating the slide.

$14 \cdot 9 = 126$ tissue specimens one by one. The challenge with scanning each region one by one is that the samples are often not equally spaced, and a lot of manual error prone labor is required to define the areas to scan. The method in this thesis tries to simplify the scanning process and prepare the images for further analysis.

The thesis are written with focus on two parts, namely automating the collection of images and correlating samples to clinical data. How this can be used in supervised machine learning will be briefly mentioned in the end. In total the method described should enable researchers to run experiments on large datasets of tissue microarrays in a structured and determined manner.

A reader of this text should be familiar with general physics. Matters that are specific to scanning microscopy and image processing will be described in the theory section, along with software concepts in use. The method section seeks to make the reader able to replicate the experiment on any kind of microscope, but some software and solutions will be specific to the Leica SP8 microscope. The result section will mark out leverages gained with automated scanning, and the discussion holds details on choices made when developing the method and limitations stumbled upon.

All source code in the thesis will be in the programming language Python⁴. The reader does not need to be proficient in Python programming, but acquaintance with the syntax is assumed. Code blocks will be used to clarify how problems have been solved or algorithms have been implemented. Details not essential to the problem at hand have been omitted to keep focus on the essential parts. As total amount of source code are above thousand lines it's not included in the appendix but rather available at [github](#)^{???} with full history. A brief description on installation of the software is included in the appendix.

As this thesis mainly consists of work on developing automated microscope scanning, the method is also the result of the thesis and therefore a result chapter is not included.

Chapter 2

Theory

Tissue microarrays

A tissue microarray is a collection of specimens arranged in a matrix pattern. The specimens are typically sliced with microtome from a paraffin block containing cylinders of tissue in rows and columns. Cylinders for the paraffin block are often picked out by a pathologist who evaluate the histology of a larger tissue sample and choose appropriate locations.

The thickness of slices are in the magnitude of $1\text{ }\mu\text{m}$, which gives efficient use of tissue samples in the sense that several hundred TMAs can be made from a block containing cylinders of height 1 mm^5 . In this text specimen spot will refer to a single sample in the array.

Scanning microscope

Figure 2.1 illustrate the internal workings of a Leica SP8 scanning microscope which have an epi-illumination setup. Epi-illumination is when the detectors (26) and light source (1, 3, 5, 7) are on the same side of the objective (18). But as seen, the epi-setup also allows for external detectors (19), which were the ones in use. By scanning one means that the light source is focused to a specific part of the specimen, scanned line by line in a raster pattern. While the laser is scanned over the surface, a detector measure light in regular time intervals (samples) and each measured sample will be saved to an image pixel.

A *photonmultiplier tube* (PMT) is a sensor that measure photons in volts. The tube works by accelerating electrons that have been liberated from an electrode by incoming photons. The electron shower is multiplied several times by arranged electrodes inside the tube, resulting in an amplification which makes it possible to measure small amounts of light.

The scanning is done by a oscillation mirror (14). The term non-descanned detector indicate that the light does not travel by the scanning mirror before reaching the detector. In SP8 (17) and (19) are non-descanned detectors, where (17) measure reflected light and (19) measure transmitted light. In figure 2.1 the condensor, which gathers light for the non-descanned detector, is not illustrated, but it should be between the glass slide and the non-descanned detector (19).

The view field of a microscope is the physical area which fits inside one image. The view field depends on the magnification of the objective and the scanner zoom. Scanner zoom is when the scanner is set to oscillate with less amplitude while still sampling at the same rate. As field of view is at the magnitude of 1×10^{-4} m, specimen must be moved around to image a larger area. The device that moves the specimen is called a stage. Here stage position, or specimen position if you like, is denoted with a upper case X to distinguish it from lower case x which denote image pixel position.

The resolution of a conventional light microscope is given by the objective and/or condensor numerical apterture (NA)⁷:

$$d = \frac{1.22\lambda}{NA_{condensor} + NA_{objective}}. \quad (2.1)$$

Here d is the minimum separable spatial distance defined by the Rayleigh criterion, λ is the wavelength of the light and NA is the numerical apterture.

A dichroic mirror, or also called a dichromatic beamsplitter, is a filter which is putted into the laser beam at 45° angle to split light of different wavelengths. The filter has a sharp transition between reflecting and transmitting light for a given wavelength, resulting in short wavelengths being mirrored 90° and high wavelengths pass through⁷. This is useful when having several detectors which should detect different wavelengths.

Second harmonic generation (SHG) is a nonlinear scattering process of two photons with the same wavelengths. The process is an interaction where the photons is transformed to a single emitted photon of half the wavelength. The process is dependent on orientation of electric dipoles in the specimen and aligned assemblies of asymmetric molecules usually provides the proper conditions. Collagen tissue does hold the proper conditions for SHG-imaging⁷.

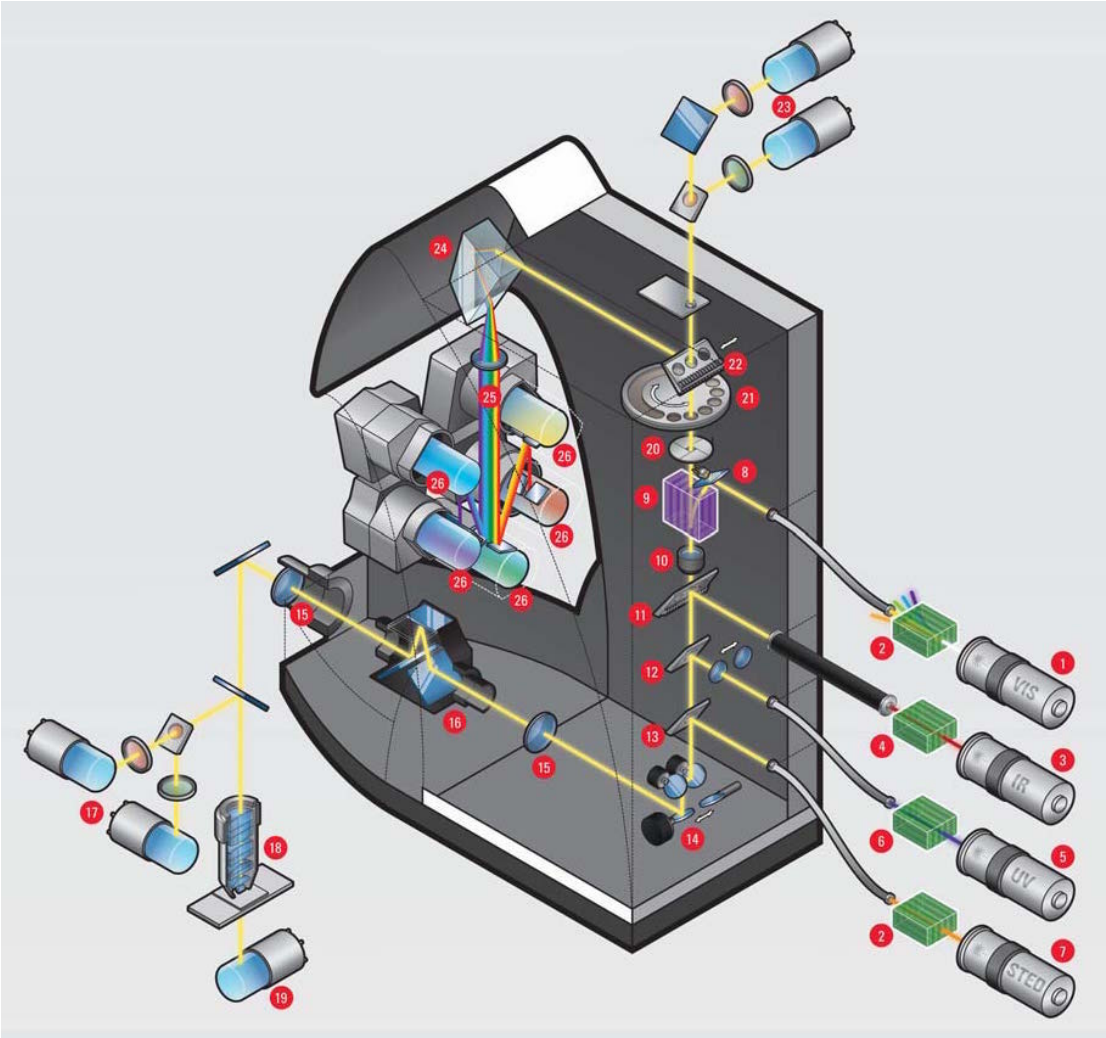


Figure 2.1: Internals of a Leica SP8 microscope. Picture from Leica SP8 brochure⁶.

As the probability for SHG is extremely low, enormous amount of light is necessary to generate it. This fact is a benefit for scanning microscope that only the focal point is able to produce SHG, with the consequences that a sensor can be simpler, e.g., non-descanned, as light will always originate from where the laser is pointed to.

SHG necessary? Not sure if I should focus on overview images only, as I have limited SHG data.

Image processing

The term image in this context is a two dimensional array of values, where each position in the array is called a pixel. Resolution is the number of pixels an image holds. E.g., a resolution of 1024x1024 is an image with 1024 pixels in both x- and y-direction, totalling 1×10^6 pixels. Each pixel represents a physical position of the specimen, where the value is the amount of light measured from the detector when scanning the specimen surface with a light source. The physical size of the pixel will depend on sampling rate. All images in this thesis are 8 bit grayscale images, meaning that each pixel can hold $2^8 = 256$ values. In an ideal experiment a pixel value of zero denotes zero detected light and 255 is the maximum, but this is an simplification as noise will be measured too.

$f(x, y)$ denotes the intensity of pixel at position (x, y) , where $(0, 0)$ is the top left of the image, positive x-direction going right and positive y-direction going down. $m \times n$ will denote the number of pixels in respectively x- and y-direction. A subscript of the image name is used if several images are discussed, e.g., m_f is the number of x-pixels of image $f(x, y)$.

The histogram of an image is the count of intensities in the image. In example, an image with 8 bit depth spans values from 0 to 255 and the histogram will have 256 bins. The 0-bin will contain the sum of pixels equal to zero in the image. Summing up all the histogram bins will give total number of pixels in the image.

Otsu thresholding

Otsu thresholding optimizes the between-class variance in terms of intensity values⁸. The computation is done on the image histogram, giving the optimal threshold for separating intensity classes. The output is a segmented binary image where all pixels above the threshold are true and the rest of the pixels are false.

Spatial image filters

A spatial image filter consists of a center pixel, it's neighborhood defined by a structuring element and a operation⁸. Structuring element is typically a rectangle, but can be of any shape. The operation can for example be calculating the mean of the neighborhood, assigning the mean value to the center pixel. Formally the spatial filter is defined as

$$g(x, y) = \sum_{s=-a}^a \sum_{t=-b}^b w(s, t) f(x + s, y + t). \quad (2.2)$$

Here $g(x, y)$ is the result, $w(x, y)$ is the structuring element, $f(x, y)$ is the image the filter is performed on and assuming odd size of the structuring element, $a = (m_w - 1)/2$ and $b = (n_w - 1)/2$.

In the case of a mean filter with neighborhood or 3×3 , $w(x, y)$ would consist of 3 rows and 3 columns with the value $1/9$.

Sliding window filters

Sliding window filters are similar to spatial filters in the sense that they look at neighboring pixels of a center pixel. The window will be all pixels surrounding the center pixel defined by the size of the structuring element. A histogram of the values in the window are updated instead of doing computation directly with the values. The histogram is efficient updated by removing the values going out of the window and adding the values coming into the window when moving to the next pixel. The result is less strain on memory access when computing the result.

Image registration

Image registration is the process of putting images into the same coordinate system. In this context the sources are images from different microscope stage coordinates. One way of finding how images are relatively displaced is by using cross-correlation. Cross-correlation two images is done by zero-padding one of the images and using the other image as structuring element. The cross-correlating $f(x, y)$ by $g(x, y)$ is defined as

$$h(x, y) = f(x, y) \star g(x, y) = \sum_s \sum_t g(s, t) f(x + s, y + t). \quad (2.3)$$

Here $g(x, y)$ is the structuring element of size $s \times t$ and $f(x, y)$ is the zero-padded image. The structuring element in cross-correlation is often called a *template* and the process of cross-correlation is called *template matching*. The maximum peak(s) in $h(x, y)$ will be where the template has the best match, which may be in several positions if several matches are made. The cross-correlation will be dependent on intensity variations and requires the images to have high entropy to get clear matches. E.g., a strictly even background have low entropy and gives equal match for the whole image⁸.

If $f(x, y)$ and $g(x, y)$ are large images, calculation of equation 2.3 is computational costly. To reduce the calculation one might use the cross-correlation theorem which uses Fourier transform to reduce number of calculations. A 2D discrete Fourier transform (DFT) of an image $f(x, y)$ is computed by

$$F(u, v) = \mathfrak{F}\{f(x, y)\} = \sum_{x=0}^{m-1} \sum_{y=0}^{n-1} f(x, y) e^{-i2\pi(ux/m + vy/n)}. \quad (2.4)$$

Here $F(u, v)$ is the frequency domain image and $\mathfrak{F}\{f(x, y)\}$ is the notation for the Fourier transform of $f(x, y)$.

Similar the inverse Fourier is defined as

$$f(x, y) = \mathfrak{F}^{-1}\{F(u, v)\} = \frac{1}{mn} \sum_{u=0}^{m-1} \sum_{v=0}^{n-1} F(u, v) e^{i2\pi(ux/m + vy/n)}. \quad (2.5)$$

The sums of equation 2.4 are independent and can be separated in rows and columns, yielding the fast Fourier transform which reduces the calculation complexity from $O(mn)$ to $O(m \log m + n \log n)$ ⁸.

As briefly mentioned, DFT has the property that a element wise multiplication in the frequency domain with one of the images complex conjugated is equivalent as a cross-correlation in the real domain. The cross-correlation theorem states

$$f(x, y) \star g(x, y) = \mathfrak{F}^{-1}\{F^*(u, v)G(u, v)\}. \quad (2.6)$$

Here it's assumed that images are zero padded and $F^*(u, v)$ denotes the complex conjugate of $F(u, v)$. Cross-correlation in the frequency domain is also called phase correlation.

Software

Leica LAS

Leica Application Suite (LAS) is the software that controls the SP8 microscope. LAS comes with a function called *Matrix Screener*, which allows the user to define structured areas to scan. The software uses the concepts fields and wells. A field is essentially an image, and a well is a collection of regular spaced images. The wells may be regular spaced, or an offset between wells can be defined in the graphical user interface. When the scan job is started Leica LAS will store images in a tree of folders in TIFF format.

CAM

In addition to controlling the microscope with the graphical user interface, a function called *Computer Assisted Microscopy* (CAM) can be turned on. CAM is a socket interface, meaning one sends bytes over a network interface. This is very similar to how one can write bytes to a file, but in addition the socket interface can respond and send bytes back. The network interface runs on TCP port 8895 and one may communicate locally or over TCP/IP network. A set of 44 commands are available, but only three of them are interesting for the purpose of controlling scans; load, autofocusscan and startscan. More details on the interface can be read in the manual⁹ or by studying the source code of the Python package leicacam¹⁰. Code block 1 shows how one can communicate with the microscope in Python.

Code block 1 Communicating with the Leica SP8 microscope using the Python package leicacam.

```
from leicacam import CAM

cam = CAM()                                # connect to localhost:8895
cam.load_template('leicaautomator')         # load a template named leicaautomator
cam.autofocus_scan()                       # start autofocusing
cam.start_scan()                           # start scan job
relpath = cam.wait_for('relpath')           # response from microscope with filename
cam.wait_for('inf', 'scanfinished')         # wait until scan is done
```

Scanning Template

A scanning template is a XML-file which defines which regions a scan job exists of. The structure of the file is the following:

- **./ScanningTemplate/Properties** holds experiment settings like start position, displacement between fields and wells, start position, which Z-drive to use, and so on.
- **./ScanFieldArray** holds all fields (images) and their settings as attributes in **./ScanFieldArray/ScanFieldData**.
- **./ScanWellArray** holds all wells (collection of images) and their settings as attributes in **./ScanWellArray/ScanWellData**.

OCR

Optical character recognition (OCR) is recognition of characters in an image. OCR internals are not discussed, but it basically works by looking at patterns in the image to convert it to text.

OCR: keep, remove or expand?

Image formats

Image formats referred to in this text are:

- *Tagged Image File Format* (TIFF) is ISO standardized¹¹ and can contain both raw and compressed images. TIFF images can be opened in most image programs.
- *Portable Network Graphics* (PNG) is both ISO and W3 standardized¹² and store images with lossless compression. PNG images can be opened in most image programs.
- *Leica Image Format* (LIF) is not a standardized format. LIF can be opened by several programs for scientific image processing (e.g., LAS, Matlab and Fiji).

Chapter 3

Methods

TMA samples can contain up to 1000 samples for each glass slide⁵. Though the complexity can be handled by a human, the process of manually scanning TMA consist of a lot error prone work. Good tools to organize the work of scanning TMAs is therefor vital in helping the researcher.

The methods described here seek to provide those tools, reducing mental overhead for the microscope operator being the main aim. Using the methods described, the user avoids a lot of repetitive trivial labor and can turn his focus on the research. In particular a detailed description of microscope settings, steps of automated scanning and correlation to clinical data follows.

Microscope

The images were collected with a Leica SP8 microscope using LAS software version X 1.1.0.12420 from Leica Microsystems CMS GmbH. Two lasers were used, a pulsing Coherent laser and a continious LASOS argon laser. Full specifications of lasers are in table 3.1.

Table 3.1: Lasers

Brand	Model	Specifications
Coherent	Chameleon Vision-S	Modelocked Ti:Sapphire, wavelengths 690-1050 nm, 2500 mW, 80 MHz pulsed repetition rate, ≈ 75 fs pulse width

Brand	Model	Specifications
LASOS	LGK 7872 ML05	Argon Continious wave, wavelengths 458, 476, 488, 496 and 514 nm, 65mW

All images are from transmitted light measured with non-descanned detectors. The non-descanned PMT detectors were used with dichrioc mirror of 495 nm and band pass filters of 525/50 nm and 445/20 nm. Rotation of scanning pattern was set to 1.7° to align scanning coordinate system with stage coordinate system (read more in Stitching). Frequency of scanning mirror was set to 600 lines/second (maximum speed with 0.75 zoom).

Images were saved as TIFF with 8 bit intensity depth and then converted to PNG to reduce storage space. The images were also rotated 270°, as LAS stores the TIFF-images with axes swapped with regards to the stage axes. The procedure is listed in code block 4.

Code block 4 Compress and rotate images.

```
from leicaexperiment import Experiment
from PIL import Image

experiment = Experiment('path/to/experiment')
experiment.compress(delete_tif=True) # lossless PNG compression

for filename in experiment.images:
    img = Image(filename)
    img = img.rotate(270)             # image axes same as stage axes
    img.save(filename)
```

Overview images

Overview images were collected with a technique similar to bright-field microscopy except that the light source is a scanning laser. 10x air objective along with argon laser in table 3.1, 514 nm emission line was used. Output power was set to 2.48% and intensity to 0.10. Forward light was imaged using 0.55 NA air condensor with non-descanned PMT detector and 525/50 nm bandpass filter.

The aperture of transmitted light and the detector gain was adjusted so that the histogram of intensities was in the center of the total range without getting peaks at minimum and maximum values. Zoom was set to 0.75 and image size 512x512, which gives images of $\approx 1500 \times 1500 \mu\text{m}$ and resolution of $\approx 3 \mu\text{m}$.

SHG images

SHG images was collected with a 25x/0.95 NA water objective. The pulsed infrared laser was set to 890 nm, intensity 20%, gain 40%, offset 80% and electro-optic modulator on. 0.9 NA air condensor was used and forward light was measured with non-descanned PMT detector using a 445/20 nm bandpass filter. Gain of PMT detector was adjusted so that signal spanned the whole intensity range. Aperture was set to 24 (maximum). Images of 1024x1024 pixels were saved.

Automated TMA scanning

The automated scanning aims to lift the burden of manual labor and prevent errors in the imaging process. The procedure finds specimen spots in an overview image and scans the specimen areas with wanted acquisition parameters. The process consists roughly of the steps:

1. Collecting an overview image with low magnification.
2. Segment specimen spots in the overview image.
3. Scan each specimen spot one or several times with chosen acquisition parameters (e.g., high magnification).

The steps listed above is fairly straight forward, but several instrumental and technical details are important to get a working solution. To better get an overview of the procedure, the aspects are listed here and described in further detail in it's own section.

In **step 1**, collecting overview images:

- Correcting for uneven illumination,
- adjusting scanner rotation
- and reliable stitching.

In **step 2**, segmentation:

- Discriminate specimen spots from background,
- excluding false positives
- and calculating specimen row and column position.

And in **step 3**, scanning each specimen spot:

- Calculating stage position from pixel position
- and communicating with the microscope.

Step 1: Collecting overview images

To find specimen, overview images were collected with the settings described in the microscope section above. To minimize scanning time, minimum zoom (0.75) was used, which yielded the intensity variation seen in figure 3.1 (a) and (b). The uneven illumination is unwanted mainly because of two reasons:

- Discriminating specimen intensities from background intensities with thresholding can give false positives when intensities are overlapping.
- Contrast is weakened, giving less clarity for human viewing purposes.

In addition, rotation of scanner raster pattern should be adjusted to avoid jagged stitch. The stitching mechanism will also be described, as existing solutions was found to be unreliable.

Uneven illumination

The uneven illumination in the experimental setup is illustrated in figure 3.1 (a). By assuming the intensity variation in all the pixels follow the slope of the background, equalization can be done by dividing the image by the normalized intensity profile of the background. The procedure is listed in code block 5.

Code block 5 Equalizing an image

```
equalized = img.astype(np.float)      # assure datatype have real division ability
equalized -= images_minimum           # normalize
equalized /= images_maximum - images_minimum
equalized /= intensity_profile        # equalize
equalized[equalized > 1] = 1          # clip values
```

As seen in code block 5, the image is first normalized. `images_minimum` and `images_maximum` is found by selecting the median of respectively minimum and maximum intensity of all images. Normalizing to the same range for all images is preferred to trusting local minimum and maximum which can give considerable differences to normalization between images.

`intensity_profile` is a curve fit for one of the background rows in a selected image. The row was found by calculating variance of all rows in the image and choosing the one with least variance. The user should verify that the row indeed is a background row by plotting it or viewing the image.

Figure 3.1(b) show the selected image and the row with least variance is indicated with a white line. The intensity profile is fitted to a second degree polynomial to steer clear from noise and then all images are equalized by the code in code block 5. The intensity profile with it's curve fit can be seen in figure 3.2(a).

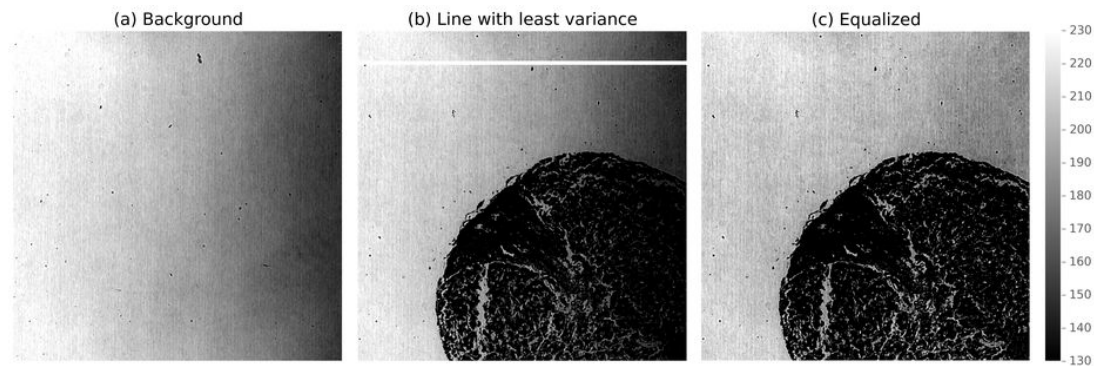


Figure 3.1: (a) Image of glass slide only for illustrating the uneven illumination. Dots are impurities on the glass slide. (b) Original image. Image is selected for finding the intensity profile. The white line is the row with least variance used for equalization. The line is higher than one pixel for viewing purposes. (c) Equalized version of (b). Note that (a), (b) and (c) are displaying values from 130 to 230 to highlight the intensity variation, colorbar is shown to the right.

The effect on pixel values can be seen in figure 3.2(b) and (c), where each dot represents a pixel value with increasing image x-position on the x-axis.

Here the intensity variation was in one dimension only, which allowed for the simpler dividing by a row intensity profile. For more complex intensity variations, similiar approaches can be done by fitting the two dimensional background to a surface, then divide images by the surface intensity profile.

Rotation

To get good stitches the microscope scanning mirror and the stage should share the same coordinate system. It's not uncommon that it does not, giving the result of a jagged stitch seen

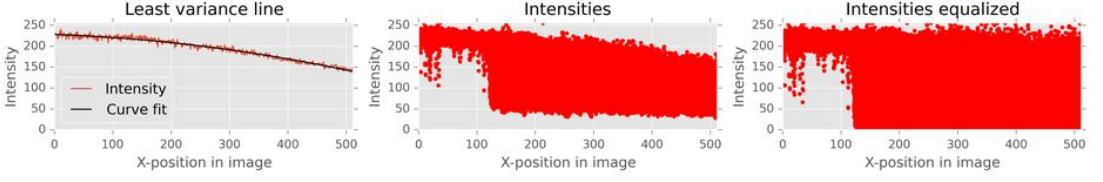
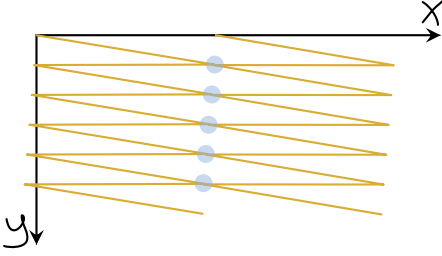
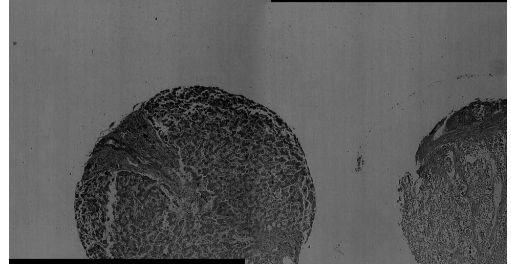


Figure 3.2: (a) Intensities for the line with least variance of figure 3.1(b). The curve is fitted to a second degree polynomial to suppress noise. (b) Intensities for image in figure 3.1(b). Each dot represents a pixel. (c) Intensities for the equalized image in figure 3.1(c). Each dot represents a pixel. Note that the intensities is both spread across the whole intensity range (0-255) and the skewness is fairly straightened out.



(a) Illustration of rotated scanning mirror coordinate system.



(b) Best stitch of two images when stage and scanning mirror does not hold the same coordinate system.

Figure 3.3: Illustrations and stitch of two images with scanning pattern rotated compared to stage movement. In (a) the first row of the first image lines up with second row in second image. The second image should therefore be one pixel above the first image. In (b) relative scanning pattern rotation is counter clockwise, giving the second image below the first image. A calculation of stage position by y-equivalent to equation ?? will give a systematic error in the y-position if stitches are jagged.

in figure 3.3.

Relative rotation between scanner raster pattern and stage coordinate system was measured by calculating displacement of two neighbor images using phase correlation. The rotation is then given by

$$\theta = \arctan \left(\frac{\Delta y}{\Delta x} \right). \quad (3.1)$$

Here Δy and Δx is the displacement in pixels between images. To align the coordinate systems,

scanning rotation was set to $-\theta$ in LAS.

Stitching

To allow whole specimen spots to be found by segmentation, overview images must be stitched together. Stitching by existing software gave unreliable results seen in figure 3.4(a) due to lack of control in translation constraints. To make sure the stitching does not fail, the method here takes the assumptions:

- Images are regular spaced.
- Images are of same size.
- Scale in edge of images are constant, e.g., translation is the only transformation between images.
- Side by side images have translation in one dimension only (see section on rotation above).

The procedure may not work well for all experimental setups, but showed good performance in regards to precision for the Leica SP8 stage.

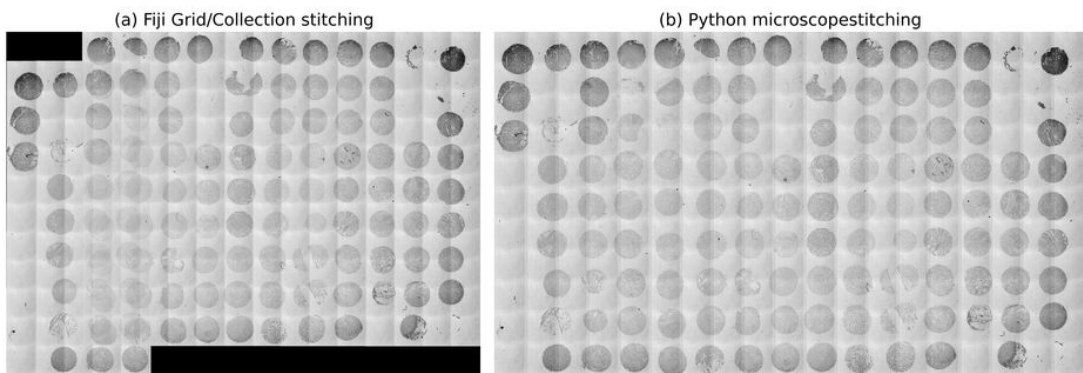


Figure 3.4: (a) Unreliable stitching with Fiji. The image translation calculated by phase correlation is chosen without adhering to displacement constraints. (b) Using same overlap for all images gives reliable stitch.

The procedure of stitching consists of phase correlating all neighbor images, calculating the median translation and using this median translation for all images. The median is used as correlation between two images with little entropy in the seam is prone to fail. More details on this matter are described in the discussion. Code block 6 show the basics of the procedure on a row of images for sake of simplicity.

Code block 6 Stitch row of images by using median translation from phase correlation.

```

from skimage.feature import register_translation
import numpy as np

# find all neighbor translations
translations = []
prev = row_of_imgs[0]                                # row_of_imgs: list of 2d arrays
for img in row_of_imgs[1:]:                          # exclude first image
    translation, error, phasediff = register_translation(prev, img)
    translations.append(translation)                 # add translation to the list
    prev = img                                       # reference to previous image
translations = np.array(translations)               # allow for slice notation
offset_y = np.median(translations[:,0])
offset_x = np.median(translations[:,1])
assert offset_x == 0, "x-offset should be zero, " \
    + "adjust the scanning mirror rotation"

# combine into one big image
y, x = img.shape                                     # assume all images are of same size
n = len(row_of_images)
total_height = n*y - offset_y*(n-1)
stitched_img = np.zeros((total_height, x))
for i, img in enumerate(row_of_images):
    y_start = i*y - i*offset_y
    stitched_img[y_start:y_start+y, :] = img

```

Step 2: Find specimen spots by segmentation

After step 1 we have a large stitched overview image of specimen spots. We would now like to classify which parts of the image that are background and which parts hold the specimen spots. Looking at figure 3.4(b) the contrast in the center of the TMA is weaker than on the edges. To improve this, the crucial observation is that background signal tend to vary less than specimen signal. This fact makes it easier to discriminate specimen spots to background by filtering the image before segmenting it with Otsu.

In addition, relying only on Otsu thresholding will give us a lot of small segments which are not specimen spots. To exclude these false positives, area size of segments were used as a classification.

Lastly, we'll want to calculate row and column of the specimen spots so that the image can be correlated to clinical data.

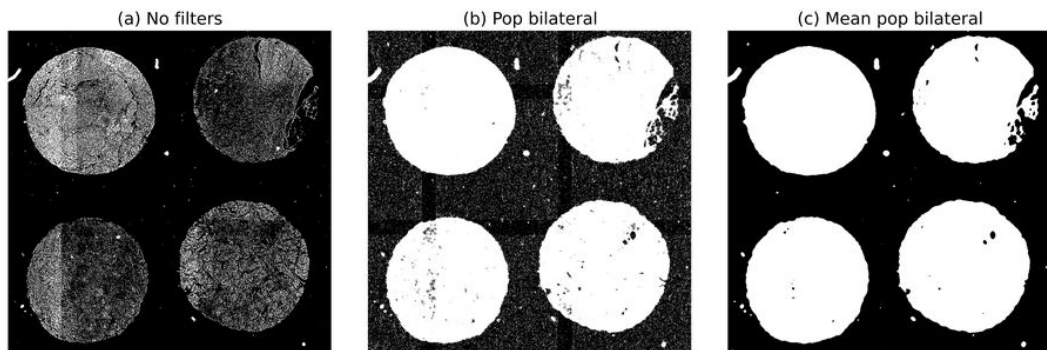


Figure 3.5: Otsu thresholding of figure 3.4(b) zoomed into four specimen spots for clarity. **(a)** Otsu thresholding applied without any filters. Picks out dark areas, but disjointed, especially for brighter areas in specimen spots. **(b)** Thresholding after a local bilateral population filter. Quite noisy in the background. **(c)** Thresholding after local bilateral population and local mean filter. Background noise is gone and sample spots are segmented continuously.

Filter and segment the overview image

As briefly mentioned, the goal of filtering the overview image is to improve discrimination between areas with background and specimen so specimen spots can be distinguished. A filter that has the appropriate characteristics is the population bilateral filter, which counts number of pixels in the neighborhood of the center pixel that is within a specified intensity range relative to the center pixel intensity.

The stitched overview image was $5122 \times 8810 = 45$ Megapixels, giving total filter time of 20 seconds with `skimage.filters.rank.pop_bilateral` on a single core of a Intel i3 2.3 GHz CPU. As the process of segmentation was implemented as an interactive graphical user interface, filter time of 20 seconds was considered unresponsive. To approve responsiveness, the filter was implemented as a sliding window filter in Python and compiled with numba¹⁴. The numba compiled filter took 4.5 seconds on a single core of a Intel i3 2.3 GHz CPU. As the microscope computer was equipped with 16 CPU cores, the filtering was parallized with dask¹⁵, giving filtering in real time.

Assuming one has an algorithm that updates the local histogram based on a structuring element, the inner computation of a population bilateral filter is given in code block 3. A full implementation of the filter can be seen in the filters submodule of leicaautomator¹⁶. Values of `s0 = s1 = 10` gave high discrimination of specimen and background on overview images collected with settings specified in the microscope section.

```
def pop_bilateral_inner_computation(histogram, val, s0, s1):
    "Returns number of pixels that are within [val-s0, val+s0]."
    count = 0
    histogram_max = histogram.size

    for bin in range(val-s0, val+s1+1):
        if bin < 0 or bin >= histogram_max: # do not try to count outside range
            continue
        count += hist[bin] # add counts in bin v
    return count
```

To reduce noise after the bilateral population filter, a mean filter was applied. The size of structure element was 9×9 pixels for both filters. Figure 3.5(a), (b) and (c) show how the segmentation is affected by the filters. Code for reproducing the steps is in code block 7.

Code block 7 Filter and segment an image with local bilateral population and Otsu thresholding.

```
import numpy as np
from skimage.filters import threshold_otsu
from skimage.util import apply_parallel # available from v0.12
from scipy.ndimage import uniform_filter
from leicaautomator.filters import pop_bilateral

selem = np.ones((9,9)) # 9x9 structuring element
filtered = apply_parallel(pop_bilateral, image, depth=4,
                        extra_keywords={'selem': selem}) # apply filter on
                                                    # all cpu cores

filtered = apply_parallel(uniform_filter, image, depth=4,
                        extra_keywords={'size': 9}) # mean filter

threshold = threshold_otsu(filtered) # get optimal threshold
segmented = filtered >= threshold # low values indicate specimen
```

Excluding false positives in segmentation

After segmentation we have a binary image as shown in figure 3.5(c). The image contains several small dots that are not specimen spots. The dots can be removed by sorting all segment regions by area size, then excluding the smallest ones. Figure 3.6(a) show segments sorted by falling area size. Code block 8 illustrate how the small segments were excluded, keeping only the largest ones.

Calculating row and column position

As specimen spots are pretty well arranged in rows and columns, calculating the specimen row and column position will lift the burden of labeling the scanned specimen by the user.

Code block 8 Exclude small segments which are false positives.

```

from skimage.measure import label, regionprops

labels = label(segmented, background=0) # background=0: exclude background
regions = regionprops(labels)           # measure region properties
regions.sort(key=lambda r: -r.area)     # sort by area size, largest first

max_regions = 126
if len(regions) > max_regions:
    regions = regions[:max_regions]     # only keep max_regions

```

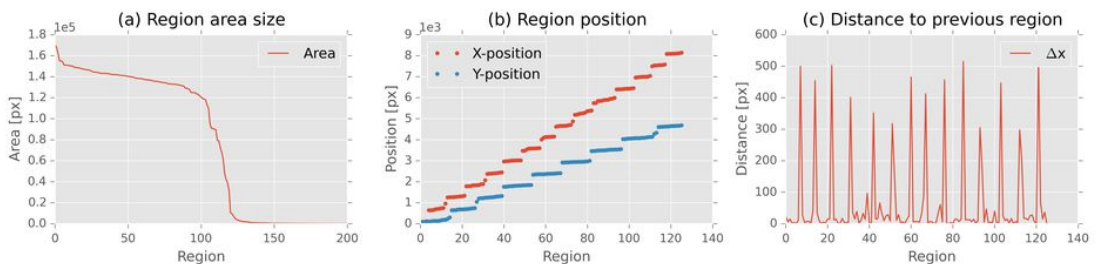


Figure 3.6: (a) Sorted region areas. Area size drops dramatically around region 125 comparable to the number of specimen spots on each slide which was $14 \cdot 9 = 126$. Plot does not have corresponding x-axis with (b) and (c), as regions are sorted by size. (b) Regions sorted by position. The two plots do not share the same x-axis. There is a gap between the positions when row and columns are increasing. (c) X distance to previous region when regions are sorted by x-position. Same x-axis as in (b) for the x-position plot. 14 peaks indicate that the image contains 15 columns.

By looking at two fairly vertical columns of specimens, one can observe that the x-coordinate of specimens group around a mean x-coordinate and that there is a jump in x-coordinate when going to the next column of specimens (seen in figure 3.6(b)). A derivative can be calculated by sorting the segmented regions by coordinate and subtract the current region's position to the previous region's position (seen in figure 3.6(c)). The derivative can then be used to increment row or column when looping through the segmented regions and adding the row and column property to the region in question. The procedure is shown in code block 9.

Interactive segmentation

As experimental factors like detector gain, laser intensity, light absorption of specimen, etc. can give considerable variations in images, step 2 was implemented as an interactive graphical user

Code block 9 Calculate row and column position to specimen spots.

```

for r in regions:
    r.y, r.x, r.y_end, r.x_end = r.bbox # for notational convenience

for direction in 'yx':
    regions.sort(key=lambda r: getattr(r, direction))

previous = regions[0]
for region in regions:
    dx = getattr(region, direction) - getattr(previous, direction)
    setattr(region, 'd' + direction, dx)
    previous = region

```

interface. The interface allows the user to adjust filter settings and verify which regions to scan by deleting, moving or adding regions. The interface is show in figure 3.7.

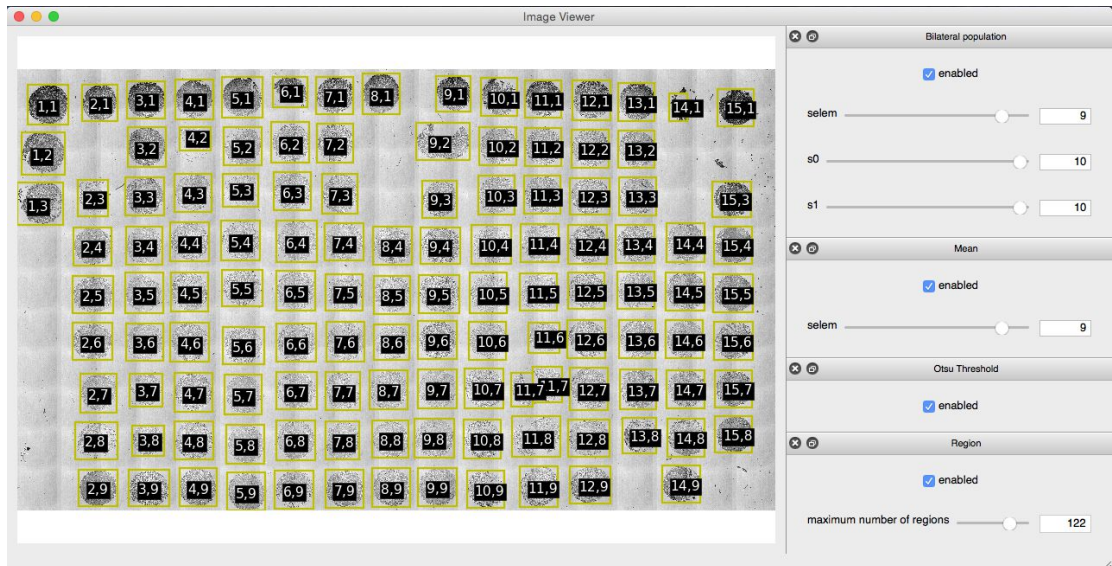


Figure 3.7: The process of segmentation in a graphical user interface. Regions 4,2, 11,7 and 14,1 might be adjusted by the user, all other regions are detected fairly well.

Step 3: Scanning each specimen spot

From step 2 we have a list of regions and their pixel position in the stiched overview image. Last step is to calculate the stage position to the regions and scan the regions by communicating with the microscope.

Calculate stage position from pixel position

To convert pixel position to stage position one need a reference point and the pixel resolution. For simplicity, the procedure for calculating stage coordinate is shown for x-coordinate only, as the calculations for y-coordinate is fully equivalent. Pixel resolution was calculated by

$$x_{resolution} = \frac{\Delta x}{\Delta X}. \quad (3.2)$$

Here Δx is displacement in pixels from the stitch in step 1, and ΔX is stage displacement in meters read from XPath `./ScanningTemplate/Properties/ScanFieldStageDistanceX` in the overview scanning template in the experiment folder (AdditionalData/{ScanningTemplate}overview.xml).

Keeping stage position constant when zooming, either by changing objective or decreasing amplitude of scanning mirror oscillation, will yield the same physical position in center of view field. This means that image stage position reported by the microscope is the center pixel. One can use the center of the first image as the reference point, but using pixel (0,0) is simpler as one can find out where the center pixel is one time, then later forget about it.

In other words, the reference point for x-position is at $f(0, y)$, the left most pixel. This reference point was calculated by

$$X_{ref} = X_{center} - \frac{m}{2} \cdot x_{resolution}. \quad (3.3)$$

In equation 3.3 X_{center} is the stage position for the top left image, m is the number of pixels in the image and $x_{resolution}$ is from equation 3.2. X_{center} was read from XPath `./ScanFieldArray/ScanFieldData[@WellX="1"][@WellY="1"][@FieldX="1"][@FieldY="1"]/FieldXCoordinate` in the overview scanning template.

The stage x-coordinate for any pixel is then given by

$$X = X_{ref} + x \cdot x_{resolution}. \quad (3.4)$$

Here X is the stage x-coordinate, X_{ref} is the reference point and $x_{resolution}$ is from equation 3.2.

As moving to the position calculated from equation 3.4 will center the location in the field of view, one need to reverse equation 3.3 if one only want this position to be included in the image and not centered in the image. How much one need to add depends field of view in the scan

job, given by the objective and the zoom defined. The start coordinate of the scan is therefore calculated by

$$X_{start} = X + \frac{\Delta X_{job}}{2}. \quad (3.5)$$

Here X_{start} is the x-coordinate for the first image, X is calculated from the bounding box coordinate to the region in question, and X_{job} is stage displacement between fields. Similar to equation 3.2, X_{job} was read from `./ScanningTemplate/Properties/ScanFieldStageDistanceX`, but in the job scanning template.

Using the stage displacement gives an error in the calculation of X_{start} by

$$\epsilon = \frac{1}{2}(\Delta X_{job} - \Delta X_{img}), \quad (3.6)$$

as stage displacement X_{job} is not strictly equal to the field of view X_{img} when images are scanned with overlap. This was considered neglectible as $\Delta X_{job} \approx \Delta X_{img}$ and number of scanned fields was calculated by

$$F_x = \lceil \frac{\Delta X}{\Delta X_{job}} \rceil, \quad (3.7)$$

which is a slight overestimate. In equation 3.7 F_x is number of fields in x-direction, ΔX is size of region and X_{job} is displacement between fields.

Scanning each region

After the step above one have start position X_{start} and number of fields to scan F_x . What remains is communicating with the microscope and record output filenames of the scans.

To avoid unnecessary long stage movements between rows or columns, regions was looped through in a zick-zack pattern, given by their row and column position. For each region the scanning template was edited, the template was loaded and the scan was started through CAM. Single scanning templates was used due to a Leica LAS software limitation; scanning templates with irregular displaced wells is not supported. Code block 10 illustrates the scanning procedure.

Code block 10 Automated scanning of regions with CAM.

```

from leiscanningtemplate import ScanningTemplate as ST
from leicaautomator import zick_zack_sort
from leicacam import CAM

cam = CAM() # instantiate connection to microscope

# regions sorted as [r(1,1), r(1,2), r(2,2), r(2,1), r(3,1), r(3,2), ...]
# here r(2,1) is region(col=2, row=1)
regions = zick_zack_sort(regions, ('well_x', 'well_y'))

tmpl_path = r"C:\Users\TCS-User\AppData\Roaming\Leica Microsystems\LAS" \
            + r"\MatrixScreener\ScanningTemplates" + "\\\"
tmpl_name = tmpl_path + '{ScanningTemplate}leicaautomator'
for n, region in enumerate(regions):
    tmpl = ST(tmpl_name + str(n%2) + '.xml') # alternate between tmpl_name0/1.xml
                                           # LAS cannot load same filename twice

    tmpl.move_well(1, 1, region.real_x, region.real_y) # start position for first field
    tmpl.write() # save scanning template
    cam.load_template(tmpl.filename) # load scanning template into LAS
    cam.autofocus_scan() # do autofocus
    cam.wait_for('inf', 'scanfinished') # wait for autofocus to finish
    cam.start_scan() # run scan job
    region.experiment_name = cam.wait_for('relpath')['relpath'] # record output filename
    cam.wait_for('inf', 'scanfinished') # wait for scan to finish

```

Alignment of z-plane

The samples in figure 1.1 are 5 μm thick and keeping the sample plane at same distance from . A movement of 1.7 mm will shift columns by one, which describes the accuracy required.

Correlating images with patient data

Each TMA glass slide contains samples from 42 patients, meaning that there is three specimen spots for each patient. The slides are numbered and specimen spots on all slides are given identifiers. Figure 3.9 illustrates some of the identifiers for slide one (TP-1, tumor peripheral one), called a slide map. As seen, the identifiers consists of two numbers. The first number is the patient identifier and the second number is the sample number. The patient identifier is not incrementing systematically, so the slide maps was scanned to read out the identifier for each position.

Before the slide maps were read with OCR, they were filtered to include only text inside circles.

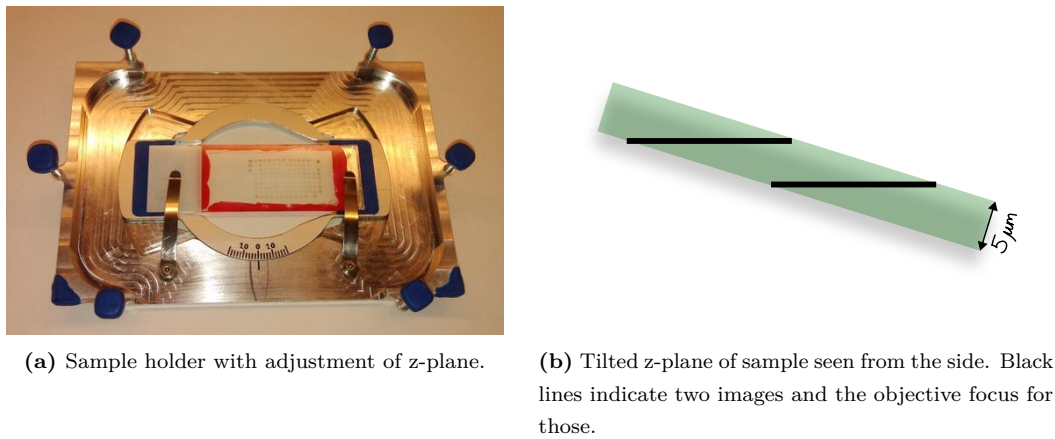


Figure 3.8

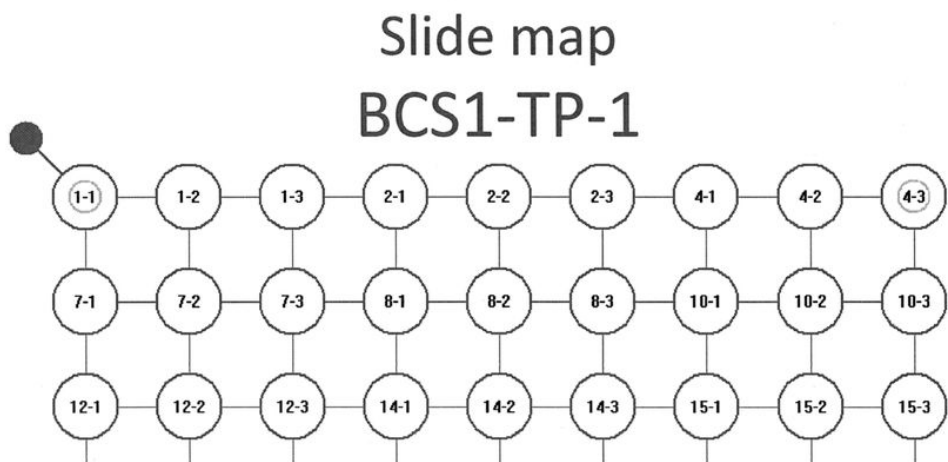


Figure 3.9: Top of slide map TP-1. Identifiers are not incrementing systematically and are inside circles, making them hard to read directly with OCR.

- Segment the image with Otsu threshold.
- Widens segments by dilation (make sure segmentation connects lines).
- Selects circles in the segment by using a circle score.
- Masks the slide map image showing only parts inside selected circles.

```
def circle_score(r):
    y0,x0,y1,x1 = r.bbox
    height = y1-y0
    width = x1-x0
    radius = (r.convex_area/3.14)**0.5
    score = 10-abs(height-width)
    score += 10-abs(radius - height/2)
    if r.area < 5000 or r.area > 8000:
        score -= 20
    return score
```

```
import numpy as np

from skimage.morphology import binary_dilation
from skimage.measure import label, regionprops

thresh = filters.threshold_otsu(img)      # segment image with Otsu thresholding
binary = img <= thresh
selem = np.ones((3,3))
binary = binary_dilation(binary, selem)   # enhance lines
labeled = label(binary)                   # find connected segments

mask = np.zeros_like(img, dtype=np.bool) # create mask of circles in image
for r in regionprops(labeled):            # for every segment
    if circle_score(r) > 0:               # circle found
        y,x,y1,x1 = r.bbox               # for notational convenience
        m = np.index_exp[y:y1, x:x1]    # where circle is found
        mask[m] = r.convex_image          # use the convex image as mask
```

```
img[-mask] = 255                                # set all pixels except contents of
                                                # circles to 255 (white)
```

After the filtering, Prizmo¹⁷ was used to read the slide maps. The OCR text output was error checked programatically for the following:

- Identifier should be of correct format.
- Identifier should increment.
- Patients should be registered with correct slide in database column TP_nr.
- Each patient should have three samples.

OCR errors was fixed manually and other errors was recorded (see section Slide map errors in the appendix).

Every patient identifier from the slide map was saved to a Stata database along with its slide number, row and column. A database with outcomes of was supplied, and code block 11 show how the clinical data can be correlated with specimen spots.

Code block 11 Get patient outcome of sample on TP-1 row 3 column 5.

```
import pandas as pd

locations = pd.read_stata('data/ids/locations.dta')    # read databases
clinical_data = pd.read_stata('data/clinic_data.dta')

condition = (locations.TP_nr == 1) & \               # position query
            (locations.TP_rad == 3) & \
            (locations.TP_kolonne == 5)

patient_id = locations[condition]['ID_deltaker']      # get patient id
assert len(patient_id) == 1                          # 1 patient registered at row/col

condition = clinical_data.ID_deltaker == patient_id.iloc[0] # clinical data query
outcome = clinical_data[condition]['GRAD']           # get outcome
```

Chapter 4

Discussion

What to communicate: discuss results, limitations, possibilities for improvement

ML: Hvilke valg har blitt tatt, hva er viktig for neste bruker, hva er begrensninger, utviklingsmuligheter, pros/cons, hvor bra fungerer det. . . .)

The glass slides in this discussion holds 14 columns of specimen spots, which is 60 non-overlapping images with a 25x objective. This means that an operator of the microscope must keep track of the current stage position in the array with limited field of view.

Automated scanning is a low hanging fruit because we have the conditions:

- Specimen spots in TMA are relatively easy to discriminate to background.
- Tissue is somewhat aranged.
- Tools in microscope software exists for controlling a scan.

Scanning

To illustrate the pros of using the method described in this thesis, lets compare it to the manual approach. By using LAS matrix screener, the procedure will be fairly structured. The manual labor in the scanning would roughly consist of:

1. Count number of rows and columns.

2. Align TMA in microscope.
3. Measure average inter sample displacement.
4. Find the maximum sized specimen spot and measure it's size.
5. Define an experiment holding the correct number of rows, columns, displacement between samples and sample size.
6. Update inter sample offsets one by one.
7. Potetially disable fields on specimen spots with smaller size than the largest.
8. Potentially identify and rule out missing samples.
9. Make sure autofocus positions will hold signal (e.g., specimen spot should be in the autofocus image).
10. Scan.

The procedure was tested out and step 6 was the most labor intensive, browsing through 126 samples aligning them. An alignment of one sample took about 40 seconds, giving 1.5 hours of intensive click-and-adjust. Also, an error in some of the steps can potentially disrupt steps further down the line, making the procedure even more labor intensive. In example, inaccuracy in average displacement between samples will lead to displacement adjustment of many wells, accidentally bumping the sample holder could impose restart of the procedure, and so on.

A simple means to avoid some of the steps in the intricate procedure above is using a single scan containing the whole matrix area. The procedure then simplifies to:

1. Align TMA in microscope.
2. Find outer boundaries.
3. Create predictive focus map or define autofocus for more or less regular spaced intervals containing a specimen spot.
4. Scan.
5. Separate specimen spots in images and assign row and column to them.

Compared to the first procedure listed, this procedure have the advantage of being less labor intensive when on the microscope, but manually browsing through $24\text{ mm} \cdot 15\text{ mm} / (400\text{ }\mu\text{m})^2 = 2250$ images may be a daunting task without a specialized tool.

The main concern with the last procedure was focus and a couple of scans confirmed the concern by having out of focus portions. The out of focus can be of several reasons, e.g., inter specimen z-displacement or temperature changes moving the specimens in z-direction. As the autofocus

in LAS runs before the scan, the only way to tackle temperature changes is by chopping up the scan in several chunks. As the goal was to reduce manual labor, doing this as a part of the procedure was not considered viable.

In other words, the most likely way to get desired result is by using the first procedure listed. So most part of the procedure was automated and the method described is therefore a combination of the two procedures above. Several of the steps remain the same but automated, so the procedure for the user of the microscope reduces to:

1. Align TMA in microscope.
2. Find outer boundaries for overview scan.
3. Verify that the algorithms have picked out the specimen spots.
 - If not, the user may adjust filter settings or directly edit the detected regions.
4. Scan.

This was considered to meet the goals; reduce mental overhead when collecting images from TMA glass slides.

Rotation

LAS comes with a interactive graphical user interface for calibrating the scanning rotation. When using the function a live image is shown, a line is drawn in the middle of the image and one can adjust the rotation while moving the stage. A reference point should then follow the line if the scanning mirror and stage holds the same coordinate system. The user himself have to find the rotation in a inductive manner by counting pixels or measuring how far the reference point moves away from the line when moving the stage. Accuracy will depend on how easily the reference point is distinguished from the rest of the image and how thoroughly the user is with his measurements. In comparison, the procedure described in the rotation section of the method gives the same precission in less time.

Images and stitching

The LAS matrix screener has two options for storing images, in TIFF or `.lif`-format (Leica image format). TIFF exporting has the advantage that it's fully controllable trough the CAM interface,

as LAS will report filenames of images when scanning. In contrast, with the `.lif`-format the user have to save the images manually in the graphical user interface and the format is not a wide adopted standard. Based on the pros of openness and automatization TIFF was chosen. None of the formats are readily putted together.

With 10x objective and 0.75 zoom, maximum field of view is reported as $1550 \times 1500 \mu\text{m}$. Average specimen spot diameter was $\approx 1200 \mu\text{m}$. These two facts would allow for imaging specimen spots into separate images if they were neatly arranged. This was not found out to be true for our dataset, and it would also burden the user of the microscope to measure and define a scan with correct inter specimen displacement. A more robust way is therefor to combine all images into one.

Combining images can be done in interactive manner, where a program loads images as one “moves” around. But creating this abstraction would demand for a way other programs can “talk” to the abstract image object containing all images. Therefor a simpler approach was used, stitching all images into one large image. This allows for any program that can open PNG to work with the images.

First approach on stitching was to use existing stitching software, in specific the *Grid/Collection stitching*-plugin of Fiji¹⁸. The plugins finds displacements between images by using phase correlation, and it works fairly well except for the lack of control when phase correlation fails. The failing of the phase correlation is mainly due to little entropy in the seam between images. It can be seen in figure 3.4, where the failed row have to much overlap. The failed row is a clean cut in the sense that the overlap between the images contain background only and no specimen. A background surface is quite even and will give a flat correlation in contrast to the wanted peak which express a match is found. In other words, the overlap between the images contain too little information for correlation and the match fails.

In addition to failures of phase correlation, we would also like to constrain stitch between two images to be in one dimension only. This is due to the systematic error which may occur if coordinate system of stage and scanning pattern is not the same. E.g., consider two side by side images as in figure 3.3. We know that the stage translation is only in x-direction, but the phase correlation tells us otherwise. As we want to register images into the stage coordinate system, rotation of scanning mirror is adjusted, but some minor rotation may still be experienced. This might be due stage inaccuracy, unlinearities in scanning pattern or wrong match from the phase correlation. Whatever the cause, offsetting images in dimension only gives at worst an error in X in the end of every stitch, but in case of offsetting in bot dimensions gives at worst a growing error. A way to overcome the error is by calculating X from the nearest image metadata, but

this was not looked into.

Taking away outliers in the registered translation of figure 3.4 gave standard deviation of 2.5 pixels, which in the context of overview images gives enough precision for defining the SHG scan job.

The stitching algorithm can be used with the python package `microscopestitching`¹⁹, code block 12 show an example of how to use it.

Code block 12 Stitching images with the Python package *microscopestitching*.

```
from microscopestitching import stitch
from glob import glob

files = glob('path/to/images/*')
images = []
for i, file in enumerate(files):
    # rectangle of 4 rows and len(files)//4 columns
    row = i % 4
    column = i // 4
    images.append((file, row, column))

stitched_image = stitch(images)
```

leicaexperiment

The TIFF images are stored in a folder tree with folder for *every* field. For a complete tissue microarray that is a couple of thousand folders, which easily becomes unmanageable if browsing directly. To improve the situation, files were stitched together such manage, one can use the python package `leicaexperiment` to work with files. This means that they have to be combined in some manner,

Segmentation

Stable stage insert

Leica LAS design

- user should be mainly in LAS
- automating on the side as a supplement
- load before CAM can be used
- does not load all settings from XML

Chapter 5

Conclusion

What to communicate: brief summary of the result and discussion, advice for further work

ML: Automatic imaging and segmentation of TMA has been demonstrated)... and....

Chapter 6

Appendix

Python software

The software in this thesis is written in Python due to Python's cross-platform support, simple syntax and vast scientific ecosystem. With Python one gets free access to a lot of scientific software libraries of high quality and top-level support through channels like github. As source code for most libraries are available, stepping into the nitty-gritty details can give insight in algorithms and be very educational.

Any Python package mentioned in the code blocks is install-able through pip. In example leicacam can be installed by opening a terminal and type `pip install leicacam`. The computer must have pip²⁰ and the required compilers if the package depends on compiling code. This is true for most of the software, it depends on fast algorithms implemented in compiled languages like C and Fortran.

Compiling the huge scientific libraries like numpy and scipy can take a while, so it's recommended to use a Python distribution like Anaconda^{???}. Anaconda pre-ships with the most common scientific libraries and it also contains the package manager conda which have pre-compiled packages available for most operating systems.

Slide map errors

```
TP2, row 3, col 6 - patient id missing in db: 66
```

```

TP6, row 1, col 9 - patient id missing in db: 222
TP3, row 1, col 3 - id 68, wrong TP_nr in db: 3.0 != 2.0
TP6, row 1, col 3 - id 209, wrong TP_nr in db: 6.0 != 4.0
TP6, row 1, col 6 - id 221, wrong TP_nr in db: 6.0 != 5.0
TP22, row 2, col 6 - id 130, wrong TP_nr in db: 22.0 != 3.0
TP22, row 2, col 9 - id 244, wrong TP_nr in db: 22.0 != 5.0
TP22, row 3, col 3 - id 281, wrong TP_nr in db: 22.0 != 6.0
TP22, row 3, col 6 - id 296, wrong TP_nr in db: 22.0 != 6.0
TP22, row 3, col 9 - id 309, wrong TP_nr in db: 22.0 != 6.0
TP22, row 4, col 3 - id 318, wrong TP_nr in db: 22.0 != 6.0
TP22, row 4, col 6 - id 376, wrong TP_nr in db: 22.0 != 7.0
TP22, row 4, col 9 - id 396, wrong TP_nr in db: 22.0 != 8.0
TP22, row 5, col 3 - id 413, wrong TP_nr in db: 22.0 != 8.0
TP22, row 5, col 6 - id 449, wrong TP_nr in db: 22.0 != 9.0
TP22, row 5, col 9 - id 453, wrong TP_nr in db: 22.0 != 9.0
TP22, row 6, col 3 - id 487, wrong TP_nr in db: 22.0 != 10.0
TP22, row 6, col 6 - id 493, wrong TP_nr in db: 22.0 != 10.0
TP22, row 6, col 9 - id 525, wrong TP_nr in db: 22.0 != 10.0
TP22, row 7, col 3 - id 728, wrong TP_nr in db: 22.0 != 15.0
TP3, row 9, col 6 - TP_nr not registered in db for ID_deltaker 140
TP5, row 9, col 9 - TP_nr not registered in db for ID_deltaker 251
TP9, row 10, col 9 - there should be 3 samples: ['467a-1']
TP9, row 11, col 3 - there should be 3 samples: ['467b-1', '467b-2'])
TP9, row 12, col 6 - there should be 3 samples: ['471a-1', '471a-2']
TP9, row 12, col 9 - there should be 3 samples: ['471b-1']
TP10, row 8, col 6 - there should be 3 samples: ['507-1', '507-2']
TP10, row 12, col 6 - there should be 3 samples: ['525-2', '525-3']
TP11, row 11, col 6 - there should be 3 samples: ['566-1', '566-2']
TP3, row 1, col 3 - patient id did not increment:
    ['68-1', '68-2', '68-3'] < ['102b-1', '102b-2', '102b-3']
TP4, row 1, col 3 - patient id did not increment:
    ['162a-1', '162a-2', '162a-3'] < ['163-1', '163-2', '163-3']
TP6, row 1, col 3 - patient id did not increment:
    ['209-1', '209-2', '209-3'] < ['268-1', '268-2', '268-3']
TP11, row 6, col 3 - patient id did not increment:

```

['549-1', '549-2', '549-3'] < ['552-1', '552-2', '552-3']

TP22, row 2, col 6 - patient id did not increment:

['130-1', '130-2', '130-3'] < ['3067-1', '3067-2', '3067-3']

References

1. Statistisk sentralbyrå. *Folkemengde, 1. Januar 2015*. Statistisk sentralbyrå; 2015. <http://www.ssb.no/befolkning/statistikker/folkemengde/aar/2015-02-19>. Accessed May 21, 2015.
2. Statistisk sentralbyrå. *Dødsårsaker, 2012*. Statistisk sentralbyrå; 2013. <http://www.ssb.no/helse/statistikker/dodsarsak/aar/2013-11-01>. Accessed May 21, 2015.
3. Brabrand A, Kariuki II, Engstrøm MJ, et al. Alterations in collagen fibre patterns in breast cancer. a premise for tumour invasiveness? *APMIS*. 2015;123(1):1-8. doi:10.1111/apm.12298.
4. Python Software Foundation. The official home of the python programming language. Python.org. 2015. <https://www.python.org/>. Accessed May 22, 2015.
5. Kononen J, Bubendorf L, Kallionimeni A, et al. Tissue microarrays for high-throughput molecular profiling of tumor specimens. *Nat Med*. 1998;4(7):844-847. doi:10.1038/nm0798-844.
6. Leica Microsystems CMS GmbH. Leica TCS SP8. 2014. http://www.leica-microsystems.com/fileadmin/downloads/Leica%20TCS%20SP8%20STED%203X/Brochures/Leica%20TCS%20SP8-Brochure_EN.pdf. Accessed May 22, 2015.
7. Murphy DB, Davidson MW. *Fundamentals of Light Microscopy and Electronic Imaging*. Hoboken, N.J.: Wiley-Blackwell; 2013.
8. Gonzalez RC, Woods RE. *Digital Image Processing*. Vol. 3 edition. Upper Saddle River, N.J: Prentice Hall; 2007.
9. Sieckmann F. *CAM Documentation, Matrix Screener 3 & 4*. Leica Microsystems CMS GmbH; 2013.
10. Seljebu A. Leicacam - control leica microscopes with python. 2015. <https://github.com/>

arve0/leicacam. Accessed May 22, 2015.

11. ISO. Tag image file format for image technology (TIFF/IT) ISO 12639:2004. May 2004.

12. ISO. Portable network graphics (PNG): Functional specification ISO/IEC 15948:2004. March 2004.

13. Duce D. Portable network graphics (PNG) specification (second edition). November 2003. <http://www.w3.org/TR/PNG/>. Accessed May 28, 2015.

14. Continuum Analytics. Numba. January 2015. <http://numba.pydata.org/>.

15. Continuum Analytics. Dask - parallel processing through blocked algorithms. 2015. <http://dask.pydata.org/en/latest/>. Accessed May 31, 2015.

16. Seljebu A. Leicaautomator - automatic scanning with leica SPX microscopes. 2015. <https://github.com/arve0/leicaautomator>. Accessed May 31, 2015.

17. Creaceed S.P.R.L. Prizmo. 2015. <http://www.creaceed.com/prizmo>. Accessed May 31, 2015.

18. Fiji is just ImageJ. May 2015. <http://fiji.sc/wiki/index.php/Fiji>. Accessed May 29, 2015.

19. Seljebu A. Microscopestitching - automatic merge/stitching of regular spaced images. 2015. <https://github.com/arve0/microscopestitching>. Accessed May 29, 2015.

20. Python Packaging Authority. User guide - pip 7.0.1 documentation. May 2015. https://pip.pypa.io/en/stable/user_guide.html. Accessed May 27, 2015.